

Compton scattering beyond the impulse approximation: Application to the core electrons of carbon

A. Issolah*

*Laboratoire de Minéralogie-Cristallographie, Université de Paris VI et Université de Paris VII, Tour 16,
4 place Jussieu, 75252 Paris Cédex 05, France*

B. Levy

*Groupe de Chimie Quantique, Laboratoire de Physico-Chimie du Rayonnement, Bâtiment No. 337,
Université de Paris-Sud, 91405 Orsay Cedex, France*

A. Beswick

*Laboratoire pour l'Utilisation du Rayonnement Electromagnétique, Université de Paris-Sud, Bâtiment No. 209D,
91405 Orsay Cédex, France*

G. Loupiau

*Laboratoire de Minéralogie-Cristallographie, Université de Paris VI et Université de Paris VII, Tour 16,
4 place Jussieu, 75232 Paris Cédex 05, France*

(Received 21 October 1987; revised manuscript received 5 April 1988)

The Compton profile produced by the 1s electrons of carbon has been calculated using (i) the impulse approximation, (ii) the hydrogenic approximation, and (iii) a type of Hartree-Fock self-consistent-field (HF-SCF) approximation. Significant deviations between the hydrogenic and the impulse results are found for incident photon energies below 25 keV. Between the hydrogenic and the quasi-HF-SCF results, the main difference is that the Compton defect and the maximum of the profile are much smaller when using the latter approximation. These differences are discussed in terms of simple models.

I. INTRODUCTION

The measurements of Compton profiles in solid-state physics provide significant information on the behavior of the valence electrons. In most cases, the experimental profiles can be analyzed successfully in the framework of the following approximations.

(1) The independent-electron (single-determinant wave function) and frozen-orbital (no relaxation after ionization) approximations, which amount to expressing the Compton profile as a sum of one-electron contributions.

(2) The impulse approximation, which provides a simple expression for these one-electron contributions.

The first of these approximations is justified by the fact that the Compton profile appears as the expectation value of a one-electron operator [see Eq. (2) below]. The other two approximations are justified if the energy ΔE transferred from the photon to the electron is much larger than the initial binding energy of the electron.¹

These approximations have to be combined with a choice for the orbitals representing the initial state of the electron (and the final state if the impulse approximation is not used; see, however, the theory developed in Ref. 2 where the explicit calculation of the final state is avoided). Each choice corresponds to a specific assumption on the potential experienced by the electron. The validity of this approximation is not directly related to ΔE .

In the present article we examine the effect of different

approximations in the case of the 1s level of carbon and for the experimental conditions of the measurements made recently at the "Laboratoire pour l'utilisation du rayonnement électro-magnétique" (LURE) on graphite and graphite intercalated compounds (initial photon energy equal to 12 858 eV, scattering angle of the photon equal to 135°, and energy ΔE transferred at the Compton peak equal to 500 eV).³ Since the contributions of the core electrons to the Compton profile are always present in the experimental results, they have to be taken into account when comparing theoretical and experimental values even though these electrons do not contribute significantly to the structure of the solid.

If the impulse approximation is not used, the simplest approach is obtained by using hydrogenic orbitals,^{1,4-7} i.e., assuming a potential of type $-Z^*/r$, where Z^* is some effective nuclear charge. However, it is well known⁸ that the results obtained when using such a potential are not always satisfactory. Therefore we shall also study the effect of using a Hartree-Fock self-consistent field (HF-SCF) type of potential instead of $-Z^*/r$.

II. THEORY

The general theory of the inelastic scattering which gives rise to the Compton profiles is well known [see, e.g., Ref. 9]. The main steps of this theory are the following.

If the energy range of the incoming photons is small enough (compared to the electron rest energy mc^2) the use of a nonrelativistic coupling Hamiltonian is justified. In atomic units this Hamiltonian is written

$$H_{\text{int}} = \mathbf{A}^2/(2c^2) - (\mathbf{p} \cdot \mathbf{A} + \mathbf{A} \cdot \mathbf{p})/(2c). \quad (1)$$

If the energy transferred in the scattering process is large compared to the initial binding energy of the electron, then the $\mathbf{p} \cdot \mathbf{A} + \mathbf{A} \cdot \mathbf{p}$ term is negligible. If in addition the coupling is weak compared to the initial energy of the photon, then the first Born approximation is sufficient.

Under these assumptions (which we assume to hold in the experimental conditions considered here), the differential cross section for the inelastic scattering of the photons is given by¹⁰

$$\frac{d^2\sigma}{d\Omega dE_2} = \left(\frac{d\sigma}{d\Omega} \right)_{\text{Th}} (E_2/E_1) \sum_f \left| \left\langle \psi_f \left| \sum_{j=1,N} e^{i\mathbf{K} \cdot \mathbf{r}_j} \right| \psi_i \right\rangle \right|^2 \times \delta(E_f - E_i - \Delta E), \quad (2)$$

where the following notations have been used: $(d\sigma/d\Omega)_{\text{Th}}$ is the Thomson scattering cross section; E_1 and E_2 are energies of the incoming and outgoing photons; E_i and E_f are the initial and final energies of the electronic system; ψ_i and ψ_f are the corresponding wave functions; \mathbf{K} is the vector difference $\mathbf{k}_1 - \mathbf{k}_2$, where \mathbf{k}_1 and \mathbf{k}_2 are the initial and final wave vectors of the photons; \mathbf{r}_j is the vector position of the electron j ; and N is the number of electrons. One can also define the Compton profile as^{4(a)}

$$J = K \left[\frac{d^2\sigma}{d\Omega dE_2} \right] / \left[\left[\frac{d\sigma}{d\Omega} \right]_{\text{Th}} \left[\frac{E_2}{E_1} \right] \right]. \quad (3)$$

In the independent-particle and frozen-orbital approximations it is first assumed that ψ_i can be described by a single Slater determinant. Furthermore, it is assumed that the ionization takes place independently for all the electrons so that ψ_f is a sum of Slater determinants where the (bound) orbitals φ_i of ψ_i have been successively replaced by (unbound) orbitals φ_f . Finally, all these determinants are assumed to be independent.

The energy difference between each of the final determinants and ψ_i is equal to the difference between the corresponding orbital energies $e_f - e_i$ [Koopman's theorem¹¹]. Note that e_i is not necessarily equal to the experimental ionization potential. Finally, one can thus write the Compton profile in the form¹

$$J = \sum_i J_i, \quad (4)$$

where

$$J_i = K \sum_f \left| \langle \varphi_f | e^{i\mathbf{K} \cdot \mathbf{r}} | \varphi_i \rangle \right|^2 \delta(e_f - e_i - \Delta E). \quad (5)$$

III. IMPULSE HYDROGENIC VERSUS EXACT HYDROGENIC APPROXIMATION

We compare here the Compton profiles predicted by the impulse and hydrogenic approximations in order to illustrate the way in which the impulse approximation breaks down in our case for sufficiently low values of the transferred energy ΔE . According to the discussion developed in Ref. (1), the Compton profile in the impulse approximation is obtained from Eq. (5) by assuming $\Delta E \gg -e_i$. After some algebra one gets¹

$$J_i(q_Z) = \int \int |\chi_i(\mathbf{q})|^2 dq_X dq_Y, \quad (6)$$

where $\chi_i(\mathbf{q})$ is the Fourier transform of the initial orbital φ_i and q_Z is given by

$$q_Z = \Delta E/K - K/2. \quad (7)$$

If, in addition, φ_i is approximated by an hydrogenic 1s orbital,

$$\varphi_i(r) = (Z_i^{*3}/\pi)^{1/2} e^{-Z_i^* r}, \quad (8)$$

where Z_i^* is the effective charge defining the potential, then^{4(a)}

$$J(q_Z) = 8Z_i^{*5} / [3\pi(Z_i^{*2} + q_Z^2)^3]. \quad (9)$$

The Compton profile in the hydrogenic approximation is obtained again from Eq. (5) by assuming that φ_i is given by Eq. (8) and φ_f by¹²

$$\varphi_f = (Z_f^*/4\pi^2 q_f)^{1/2} [1 - \exp(-2\pi Z_f^*/q_f)]^{-1/2} e^{i\mathbf{q}_f \cdot \mathbf{r}} \times {}_1F_1(iZ_f^*/q_f, 1, i(\mathbf{q}_f \cdot \mathbf{r} - q_f r)), \quad (10)$$

where \mathbf{q}_f is the asymptotic wave vector of the final electron. If the same effective charge Z^* is used for φ_i and φ_f one gets^{1,4(a)}

$$J(q_f) = \frac{256}{3} Z^{*6} K^3 [1 - \exp(-2\pi Z^*/q_f)]^{-1} \exp\{-2(Z^*/q_f) \tan^{-1}[2Z^* q_f / (Z^{*2} + K^2 - q_f^2)]\} \times (3K^2 + Z^{*2} + q_f^2) [(Z^{*2} + K^2 + q_f^2)^2 - 4K^2 q_f^2]^{-3}. \quad (11)$$

[Notice that the plots (exact hydrogenic versus impulse hydrogenic) in Ref. 1 are incorrect, as it has already been pointed out by Mendelsohn and Smith⁸.]

This Compton profile can also be expressed as a function of q_Z —like in the impulse approximation—by using Eq. (7), the relation between K and ΔE which corresponds to the geometry of the considered experiment, and the relation

$$q_f = [2(e_i + \Delta E)]^{1/2}. \quad (12)$$

We have determined the Compton profiles given by Eqs. (9) and (11) using

$$Z^* = Z_i^* = Z_f^* = (-2e_i)^{1/2} \quad (13)$$

and the value of e_i given by the HF-SCF calculation,¹³ viz.,

$$e_i = 11.33 \text{ a.u.} \quad (14)$$

Two significant features of the resulting profiles are seen in Fig. 1.

(i) The position q_{\max} of the peak given by the hydrogenic approximation is shifted to negative q_Z when the incident energy E_1 decreases. At high values of E_1 , q_{\max} coincides with the impulse value. The value of E_1 depends of course of the experimental conditions. If we assume a resolution of 0.15 momentum a.u., then a significant shift can be observed for E_1 lower than ~ 25 keV.

(ii) Concerning the amplitude of J_{\max} , the situation is qualitatively similar: the values given by the two approximations coincide at high values of E_1 , but the hydrogenic value decreases faster than the impulse one when E_1 decreases. If a relative difference of 10^{-3} is the smallest that can be observed, it is seen that the difference between the two methods appear for E_1 lower than a limit as high as ~ 90 keV.

It must be emphasized that these limits concern the difference between two approximate profiles (hydrogenic [Eq. (11)] and impulse-hydrogenic [Eq. (9)] approximations) and not the difference between the impulse and exact profiles. However, the two approximate profiles are obtained here with consistent approximations concerning the electronic states: the same initial state is used in the hydrogenic and impulse calculations, and the same effective charge is used in the initial and final states of the hydrogenic approximation. In other words, the same electronic potential $[-(-2e_i)^{1/2}/r]$ is used all through these calculations. It is likely then that the differences between the two computed profiles arise mainly from the additional dynamical assumptions made in the impulse approximation.

Concerning the experimental conditions under consideration here,³ we conclude that the initial energy (close to 13 keV) is below the limit of validity of the impulse approximation. This is in agreement with the fact that the transferred energy in the region of the Compton peak is not significantly larger than the initial binding energy of the 1s electron (ΔE close to 500 eV; $|e_i|$ close to 300 eV).

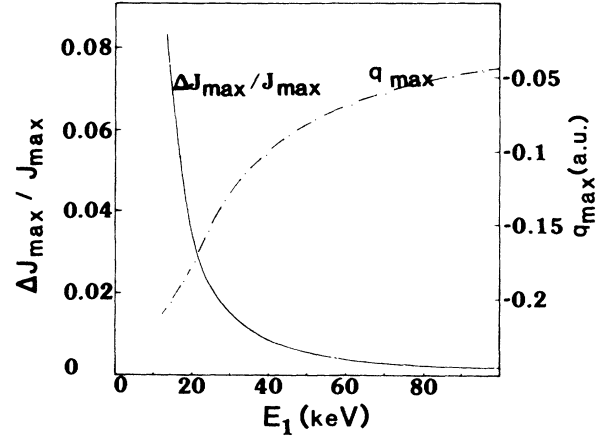


FIG. 1. Compton defect q_{\max} in the hydrogenic approximation and relative difference $\delta J_{\max}/J_{\max}$ between the maximum value of the Compton profile in the impulse and hydrogenic approximations vs the photon incident energy E_1 .

IV. HYDROGENIC VERSUS HF-SCF APPROXIMATIONS

We shall now study the difference between the Compton profile obtained in the hydrogenic approximation (i.e., assuming that the initial and final electronic states are eigenfunctions of a Hamiltonian with a potential equal to $-Z^*/r$) with the Compton profile obtained in a HF-SCF approximation.

The advantage of the hydrogenic approximation over the HF-SCF one is that it leads to simpler calculations [see Eq. (11)]. However, the hydrogenic initial state is not fully satisfactory, since it appears already in the impulse result (see Table I, methods 1 and 2, and Fig. 2).

The HF-SCF approximation does not lead to a closed expression of the profile. On the other hand, it corresponds to a more realistic potential: the HF-SCF poten-

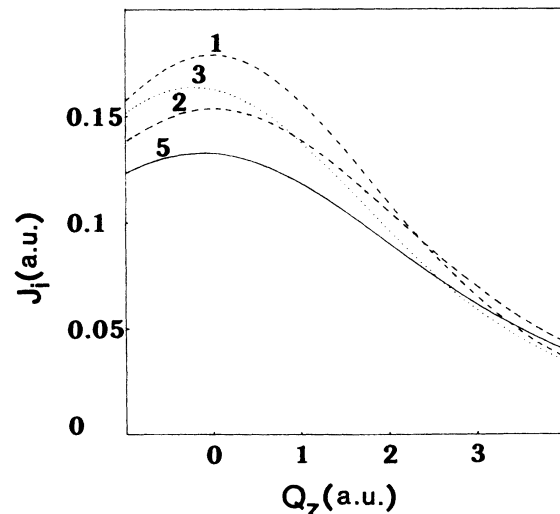


FIG. 2. Compton profiles. The number of each curve refers to the method described in Table I.

TABLE I. Summary of the values obtained here for the Compton profile of the 1s level of carbon. q_{\max} is the Compton defect, J_{\max} is the maximum value of the Compton profile, and φ_i and φ_f are the initial state and final state of the electron, respectively. The experimental conditions are described in Ref. 3. The effective charge $Z^* = 4.75931$ used in the case of the hydrogenic and Coulomb states is defined by the Eqs. (13) and (14).

Method no.	φ_i	φ_f	q_{\max}	J_{\max}
Impulse method [Eq. (6)]				
1	hydrogenic [Eq. (9)]		0	0.178
2	HF SCF		0	0.153
Nonimpulse method [Eq. (5)]				
3	hydrogenic	Coulomb [Eq. (10)]	-0.207	0.164
4	HF SCF	Coulomb [Eq. (10)]	-0.500	0.142
5	HF SCF	numerical [using the potential of Eq. (15)]	-0.112	0.133

tial for a given electron is close to $-Z/r$ (Z is the actual nuclear charge) in the region where the nuclear attraction dominates the repulsion by the remaining electrons (small r), whereas it is close to $-1/r$ in the region where the nuclear charge is screened by the charge of the other electrons (large r) instead of the same average value $-Z^*/r$ everywhere, as assumed in the hydrogenic approach.

We will analyze the difference between the Compton profiles obtained by these two methods by considering the intermediate case of a calculation using a HF-SCF initial state and an hydrogenic final state (Table I, method 4). The physical meaning of such a calculation might seem questionable: the two states are not eigenfunctions of the same Schrödinger equation and in particular they are not orthogonal. It will turn out, however, that this hybrid calculation provides useful insights (see discussion below).

V. HYDROGENIC VERSUS HF-SCF INITIAL STATE

The algebraic calculation leading to the expression of the Compton profile in the case of an HF-SCF initial state and hydrogenic final state is outlined in Appendix A. The results, obtained with the HF-SCF orbital of Ref. 13, are given in Table I (method 4).

It is seen in Table I that the resulting Compton defect

is significantly larger and the resulting maximum J_{\max} significantly smaller than the ones obtained by the hydrogenic approximation [Table 1, method 3].

In order to interpret these two features we have determined the Compton profiles in the hydrogenic case with a fixed charge Z_f^* given by the Eqs. (13) and (14) for the final state and varying values of the effective charge Z_i^* for the initial state. This is a hybrid calculation with the same type of questionable physical meaning as that of method 4. The corresponding expression of the Compton profile J_i is given in Appendix B, and the results are presented in Table II.

It is seen that increasing Z_i^* qualitatively results in the same two effects as the ones found when replacing the initial hydrogenic orbital by a HF-SCF one (method 4). A quantitative agreement can even be obtained: it is seen that $Z_i^* = 5.53$ a.u. reproduces fairly well the profile obtained in the method 4 (Compton defect equal to -0.541 and -0.500 a.u., respectively; maximum value of J_i equal to 0.143 and 0.142, respectively).

We conclude that the effect observed on the Compton profile when changing the hydrogenic initial state into a HF-SCF one can be simply described as resulting from a scaling (such as the one obtained by changing Z_i^* in the hydrogenic state) although the actual difference between the two orbitals might be more complicated.

VI. HYDROGENIC VERSUS NUMERICAL FINAL STATE

We consider here the effect of improving the potential for the final state. We have used the V^{N-1} potential,

$$V(r) = -Z/r + J_{1s} + 2[J_{2s} + (J_{p_x} + J_{p_y} + J_{p_z})/3], \quad (15)$$

where Z is the actual charge of the nucleus and the J_k are the Coulomb operators corresponding to the orbitals φ_k ,

$$J_k(r) = \int d^3r' |\varphi_k(r')|^2 / |\mathbf{r} - \mathbf{r}'|. \quad (16)$$

This potential is not the HF-SCF one since we have removed the exchange terms for convenience, but the orbit-

TABLE II. Values q_{\max} and J_{\max} obtained with the method 3 of Table I with different effective charges in the initial state.

Z_i^*	Z_f^*	q_{\max} (a.u.)	J_{\max} (a.u.)
4	4.76	0.118	0.192
4.5	4.76	-0.096	0.172
4.76	4.76	-0.207	0.164
5	4.76	-0.311	0.157
5.53	4.76	-0.541	0.143
6	4.76	-0.745	0.133

als φ_k used for computing it are true HF-SCF orbitals (determined with the exchange terms included).¹³

In fact, the main property that we require here for the potential is that it is close to $-Z/r$ for small r and to $-1/r$ for large r . This is actually the case for the potential defined in Eq. (15) as seen in Fig. 3. A similar approach has been presented in Refs. 10 and 14.

A. Determination of the final-state wave function

The final state of the Compton process is an eigenfunction of the Schrödinger equation with the potential defined in Eq. (15). In order to determine that function, we first expand it in partial waves,

$$\varphi_f = r^{-1} \sum_l C_l f_l(q_f, r) P_l(\cos\theta), \quad (17)$$

where C_l is a normalization factor, f_l a function to be determined, and θ is the angle between the q_f and r vectors. The function f_l is evaluated by a numerical integration of the corresponding Schrödinger equation on a grid of points starting at small r with the regular solution (and its derivative) corresponding to the potential $-Z/r$,¹⁵

$$f_l(q_f, r) = (q_f r)^{l+1} e^{iq_f r} \times {}_1F_1(l+1+iZ/q_f, 2l+1, -2iq_f r). \quad (18)$$

In order to determine the normalization factor C_l we first write f_l (for large values of r) in the form

$$f_l(q_f, r) = \alpha_l F_l(q_f, r) + \beta_l G_l(q_f, r), \quad (19)$$

where F_l and G_l are, respectively, the regular and irregular solutions of the Schrödinger equation corresponding to the potential $-1/r$. The coefficients α_l and β_l are determined by identifying the values of f_l and of df_l/dr resulting from the integration with the asymptotic values of F_l , G_l , and their derivative given in Eqs. 14.5.1–14.5.8 of Ref. 15.

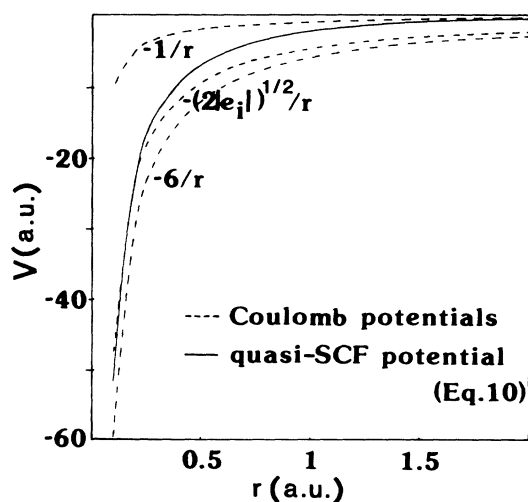


FIG. 3. Potential V in the hydrogenic approximation (dotted lines) and in the quasi-HF-SCF approximation (solid line) as a function of the distance r to the nucleus.

Then the expression of f_l given in Eq. (19) is compared with the following normalized asymptotic form [cf. Eq. 6.90 of Ref. 12]:

$$C_l f_l = A_l [H_l^-(q_f, r) + \exp(2i\Delta_l) H_l^+(q_f, r)], \quad (20)$$

where

$$A_l = (2\pi)^{-3/2} (2q_f)^{-1} (2l+1) i^l \quad (21)$$

and H_l^\pm are defined in Eq. (6.69) of Ref. 12. Finally, Δ_l is a phase shift that needs not be determined here. Using Eqs. (19) and (20) and the relation between the asymptotic forms of F_l , G_l , H_l^+ , and H_l^- [Eq. (6.72) of Ref. 12] one finds

$$C_l = 2 A_l (\alpha_l + i\beta_l)^{-1}. \quad (22)$$

B. Determination of the Compton profile

We have now to determine the Compton profile given by Eq. (5), using the functions φ_f defined on a grid of points. For that purpose we expand $e^{i\mathbf{K}\cdot\mathbf{r}}$ in partial waves and $P_l(\cos\theta)$ [appearing in Eq. (17)] as a sum of products of spherical harmonics. This gives

$$J_i(q_f) = 64\pi^3 K q_f \sum_l (2l+1)^{-1} |C_l \int dr r f_l(q_f, r) j_l(Kr) \times \varphi_{1s}(r)|^2, \quad (23)$$

where C_l and f_l are determined as explained in Sec. VI A, j_l is the spherical Bessel function coming from the expansion of $e^{i\mathbf{K}\cdot\mathbf{r}}$, and φ_{1s} is the HF-SCF $1s$ function used in Sec. V. The integral in Eq. (23) is performed numerically by a Gauss quadrature. The whole procedure for determining C_l , f_l , and J_i has been checked by using the potential $V(r) = -Z^*/r$ in the numerical integration and comparing the resulting profile with that given by Eq. (11).

VII. RESULTS

The results of the calculations presented in Sec. VI are shown in Table I (method 5). By comparing with the results obtained with method 4, it is seen that replacing the hydrogenic final state by that resulting from the potential of Eq. (15) increases the value of q_{\max} (i.e., decreases $|q_{\max}|$) and decreases J_{\max} .

It turns out that these variations of q_{\max} and J_{\max} cannot be explained by an analogy with the variations obtained when changing Z_f^* in the hydrogenic approximation. In order to demonstrate that, we have calculated the Compton profiles in the hydrogenic approximation with a fixed effective charge Z_i^* given by the Eqs. (13) and (14) for the initial state, and varying values of the effective charge Z_f^* for the final state (this is a calculation similar to that presented in Sec. V, but the roles of Z_i^* and Z_f^* are interchanged; the expression for J_i is given in Appendix B). The results are presented in Table III: it is

TABLE III. Values q_{\max} and J_{\max} obtained with the method 3 of Table I with different effective charges in the final state.

Z_i^*	Z_f^*	q_{\max} (a.u.)	J_{\max} (a.u.)
4.76	0	1.84	0.178
4.76	1	1.35	0.183
4.76	2	0.89	0.184
4.76	3	0.46	0.179
4.76	4	0.07	0.171
4.76	4.76	-0.21	0.163
4.76	5.53	-0.49	0.156
4.76	6	-0.65	0.152

seen that for $Z_f^* > 2$ the variations of q_{\max} and J_{\max} as a function of Z_f^* are parallel instead of being opposite when passing from method 4 to method 5. In addition, for $Z_f^* < 4$, the value of q_{\max} is much larger than the one found in methods 3 and 5.

Thus, in order to interpret the effect of improving the potential used for determining the final state, we have to go into a more detailed analysis of Eq. (5).

A. Variation of q_{\max}

The most important aspect of this equation, in the frame of the present discussion, is that $e^{i\mathbf{K}\cdot\mathbf{r}}$ and φ_f are oscillatory functions. For instance, if φ_f is a plane wave (hydrogenic approximation with $Z_f^* = 0$), then the matrix element in Eq. (5) is simply the Fourier transform of φ_i and the maximum is obtained when the vector $\mathbf{K} + \mathbf{q}_f$ vanishes. Thus, after integrating over the final state (i.e., over the angle between the vectors \mathbf{K} and \mathbf{q}_f), it can be expected that the maximum of J_i is obtained when the modulus of \mathbf{K} and \mathbf{q}_f are equal,

$$q_f = K \quad (24)$$

[cf. also Appendix B, Eq. (B4)], or equivalently, when

$$q_{\max} = -e_i / K \quad (25)$$

Indeed, using the actual value of K at the maximum obtained for $Z_f^* = 0$ ($K = 6.17$ a.u.) one gets from Eq. (25) $q_{\max} = 1.84$ a.u. in agreement with the actual value (cf. Table III).

When $Z_f^* \neq 0$, the relation (24) cannot be satisfied over the whole range of the integration for the matrix element of Eq. (5) (i.e., $r = [0, \infty]$). However, this might not be necessary since φ_i is a bound state and can be considered to be zero for r larger than some value r_{\max} .

Let us consider the curve in Fig. 4 giving the partial values of J_{\max} obtained with Eq. (23) and the integral over r restricted to a finite range from 0 to r_{\sup} . It is seen that here r_{\max} is close to 1 a.u.: the matching between $e^{i\mathbf{K}\cdot\mathbf{r}}$ and φ_f expressed by Eq. (24) has to be achieved only in the range $r = 0$ to $r = 1$ a.u. in order to get the maximum J_{\max} .

In addition, it is seen in Fig. 4 that the main contributions to J_i comes from a rather small interval around a mean value \bar{r} close to 0.45 a.u. Thus if we define a local momentum

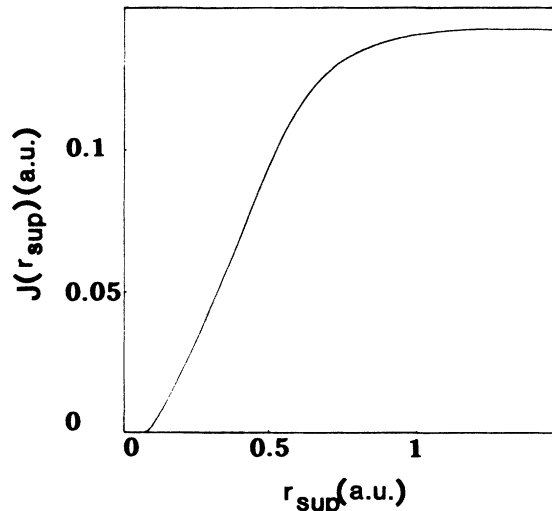


FIG. 4. Partial values $J(r_{\sup})$ of J_{\max} (in method 4) evaluated by Eq. (23) with the integral over r restricted to $(0, r_{\sup})$.

$$q_f(r) = \{2[e_f - V(r)]\}^{1/2}, \quad (26)$$

where $V(r)$ is the potential used for determining φ_f , we can reasonably replace Eq. (24) by

$$q_f(\bar{r}) = K \quad (27)$$

[This equation (27) is likely to correspond better to the actual maximum when the mismatch between $e^{i\mathbf{K}\cdot\mathbf{r}}$ and φ_f over the interval $r = [0, r_{\max}]$ is not too large.]

Equation (27) leads to

$$q_{\max} = [V(\bar{r}) - e_i] / K \quad (28)$$

This expression can be checked in different ways. Firstly, it can be seen that it predicts that q_{\max} decreases when Z_f^* increases, as actually found (see Table II). Secondly, the slope $(dq_{\max}/dZ_f^*)_{Z_f^*=0}$ is found from Eq. (27) to be equal to $-1/(\bar{r}K) = -0.36$ a.u., in reasonable agreement with the slope resulting from the values given in Table III (-0.49 a.u.). Finally, we note that the Eq. (28) explains the shift of q_{\max} when changing the potential,

$$\delta q_{\max} = \delta V(\bar{r}) / K \quad (29)$$

When passing from method 4 to method 5, this gives $\delta q_{\max} = 0.40$ a.u., in good agreement with the shift that has been actually found ($\delta q_{\max} = 0.39$ a.u., cf. Table I).

B. Variation of J_{\max}

Let us now turn to the variation of J_{\max} when passing from a hydrogenic to the quasi-HF-SCF final state (i.e., from method 4 to method 5 defined in Table I). As mentioned above, the matching between $e^{i\mathbf{K}\cdot\mathbf{r}}$ and φ_f expressed by the Eq. (24) or (27) can be achieved over the whole range $r = [0, r_{\max}]$ only if φ_f is a plane wave. Otherwise a perfect matching cannot be achieved and it seems likely that J_{\max} decreases when the mismatch increases, i.e., when the variation of $V(r)$ around the point $r = \bar{r}$ becomes steeper.

It is possible to construct a simple model that allows us to check indirectly that the variations of J_{\max} and of the mismatch between $e^{i\mathbf{K}\cdot\mathbf{r}}$ and φ_f are opposite. In order to construct this model, we first need a precise definition of the mismatch. It is directly related to the variation of $q_f(r)$ when calculating the matrix element in Eq. (5). However, the definition $q_f(0) - q_f(\infty)$ corresponding to the total variation of $q_f(r)$ is not convenient here: The range of r corresponding to $r > r_{\max}$ (r_{\max} as defined in Sec. VII A) does not contribute significantly to the matrix element; the quantity $q_f(0)$ is unbound [$q_f(0) = \infty$]. Therefore we chose to define the mismatch δq_m for a given method m and a given final state φ_f as

$$\delta q_m = q_f(r_{\min}) - q_f(r_{\max}), \quad (30)$$

where r_{\min} is some reasonable value.

The model is then completed by relating the profile J_m obtained in some method m (method 4 or method 5 in Table I) and the profile J_0 obtained with a plane-wave final state (hydrogenic approximation with $Z_f^* = 0$): we assume that the progressive setup of δq_m in the course of the calculation of the matrix element in Eq. (5) amounts to a constant mismatch δq_m in the case of J_0 . Thus the profile J_m obtained with a given final state is equal to the profile J_0 obtained with a plane wave with momentum $q_f(\bar{r}) + \delta q_m$,

$$J_m(q_f(\bar{r})) = J_0(q_f(\bar{r}) + \delta q_m) \quad (31)$$

[note that the Eq. (31) is valid only for $q_f(\bar{r}) > K$: if $q_f(\bar{r}) < K$, the sign of δq_m on the right-hand side of Eq. (31) should be inverted, otherwise J_m and J_0 would be identical apart from a shift on the q_f scale].

If we consider now two methods m and m' , the values of the corresponding profiles (corresponding to two final states φ_f and $\varphi_{f'}$) are equal if the arguments of J_0 in Eq. (31) are equal,

$$q_f(\bar{r})_m + \delta q_m = q_{f'}(\bar{r})_{m'} + \delta q_{m'}. \quad (32)$$

If we consider now the value of $q_f(\bar{r})_m$ corresponding to the maximum of J_m , viz., $q_f(\bar{r})_m = K$, then the Eq. (32) gives

$$q_{f'}(\bar{r})_{m'} = K + \delta q_m - \delta q_{m'} \quad (33)$$

[note that Eq. (33) is consistent with Eq. (31) if $\delta q_m - \delta q_{m'} > 0$: otherwise one should interchange the roles of m and m']. Using Eqs. (7) and (26) we get the value of q_z for which J_m is equal to the maximum of J_m ,

$$q_z = q_{\max}(m') + d\delta q + (d\delta q)^2 / (2K), \quad (34)$$

$$d\delta q = \delta q_m - \delta q_{m'}. \quad (35)$$

We have determined numerically these quantities when m' is method 4 and m is method 5 using $r_{\min} = 0.1$ a.u. It gives $q_z = 0.31$ a.u., which corresponds to $J_i = 0.134$ a.u. in method 4 to be compared with $J_{\max} = 0.133$ a.u. in method 5 (see Table I).

The meaning of the agreement between these two values should not be overestimated because it strongly

depends upon r_{\min} . At least the order of magnitude and the sign of the variation of J_{\max} between the two methods are accounted for.

VIII. DISCUSSION AND CONCLUSION

We have compared the Compton profile of the 1s level of carbon (corresponding to the experimental conditions of Ref. 3), obtained in a pure hydrogenic approximation (Table I, method 3) with that obtained in a quasi-HF-SCF approximation (Table I, method 5). It appears that the Compton defect is nearly the same in the two approximations, the maximum found in the latter case being slightly closer to that found in the impulse approximation than the former. This small variation of the Compton defect appears to be the result of a compensation between two larger effects: Replacing the hydrogenic initial state φ_i by the HF SCF one shifts the maximum of the Compton profile to a very negative value of q_z , because the HF-SCF φ_i is more concentrated than the hydrogenic one due to a more attractive potential at short distances of the nucleus; replacing the final state φ_f nearly brings back the maximum to $q_z = 0$ because—see Eq. (28)—the quasi-HF-SCF potential is less attractive than the hydrogenic one at intermediate distances of the nucleus. On the other hand, the maximum value of the Compton profile of method 5 is significantly smaller than that of method 3 due to two cumulative effects: The HF-SCF φ_i is more concentrated than the hydrogenic one (as mentioned for the Compton defect); the mismatch between φ_f and $e^{i\mathbf{K}\cdot\mathbf{r}}$ over the range of φ_i is larger in method 5 than in method 3 due to a steeper variation of the potential.

It is seen from this analysis that it is difficult to reproduce the results of method 5 in the frame of the hydrogenic model. Here, we have found that it would require us to use the following effective charges: $Z_i^* = 6.91$ a.u. and $Z_f^* = 2.59$ a.u. The meaning of using such different values is rather questionable from a theoretical point of view; the value of Z_i^* corresponds to $e_i = -23.87$ a.u. (instead of -11.33 a.u. for the 1s HF-SCF orbital); in addition, it seems difficult to find the values of these effective charges without previous knowledge of the results of method 5.

It has been suggested⁴ to calibrate Z_i^* on the value of J_{\max} found in the impulse approximation with the HF-SCF φ_i . Here, this gives $Z_i^* = 5.53$ a.u.; then using $Z_f^* = (-2e_i)^{1/2} = 4.75931$, it gives $J_{\max} = 0.143$ a.u., $q_{\max} = -0.54$ a.u. It is seen that J_{\max} might be considered to be reasonable, but q_{\max} is definitely too small (or too large in absolute value).

One problem in method 5 is the neglect of the exchange terms in the potential. The effect of these terms is difficult to evaluate exactly. However, the fact of neglecting them results in a final state φ_f which cannot be exactly orthogonal to the bound state. Here we have found at $q_z = q_{\max}$

$$\langle \varphi_f, \varphi_{1s} \rangle = 6.8 \times 10^{-6},$$

$$\langle \varphi_f, \varphi_{2s} \rangle = 1.2 \times 10^{-4},$$

$$\langle \varphi_f, \varphi_{2p} \rangle = 1.6 \times 10^{-3} .$$

We conclude that the exchange terms are probably not very important here. On the contrary, we have seen that using the actual Coulomb part of the potential, instead of the average corresponding to the hydrogenic model with $Z_f^* = (-2e_i)^{1/2}$, does provide improvements of the Compton profile which are significant compared to the accuracy of the present experiments.

ACKNOWLEDGMENTS

We wish to thank Dr. J. Chomilier for very helpful discussions. All the calculations presented here have been performed on the Modcomp Classic 32/85 computer of the Groupe de Chimie Quantique (Orsay).

APPENDIX A

We outline here the computational method that we have used to determine the Compton profile in the case of method 4 (Table I), where the initial state φ_i is the HF-SCF 1s orbital of the carbon atom and φ_f is a Coulomb wave corresponding to a $-Z_f^*/r$ potential. Several forms for φ_i are available in the literature using either Gaussian¹³ or 1s and 2s Slater functions.¹⁶ However, only expansion in terms of 1s Slater functions leads to a simple evaluation of the matrix element of $e^{i\mathbf{K}\cdot\mathbf{r}}$. The use of 2s Slater functions leads to a more complicated expression. Thus the simplest approach consists of fitting the initial φ_i by a combination of 1s Slater functions. In addition, the use of Gaussian functions leads to a simpler evaluation of the potential $V(r)$ defined in Eq. (15). Finally, we have used the Gaussian expansion¹³ and we have reexpressed it in a basis of 4 exponential functions with exponents obtained by multiplying $(-2e_i)^{1/2}$ (=4.75931 a.u.) successively by 1, 1.5, 2, and 2.5. The expansion coefficients of the orbital in this new basis are obtained by

a least-square fit.¹⁷

Then, using Eq. (12) of Ref. 5, one gets a closed expression for

$$M_l = \langle \varphi_c(Z_f^*, \mathbf{q}_f, \mathbf{r}) | e^{i\mathbf{K}\cdot\mathbf{r}} \varphi_{1s}(Z_l, \mathbf{r}) \rangle , \quad (\text{A1})$$

where $\varphi_c(Z_f^*, \mathbf{q}_f, \mathbf{r})$ is the Coulomb wave of asymptotic momentum \mathbf{q}_f and corresponding to the nuclear charge Z_f^* ; $\varphi_{1s}(Z_l, \mathbf{r})$ is an exponential function with exponent Z_l .

As explained above, the initial state is written here as

$$\varphi_i(\mathbf{r}) = \sum_l c_l \varphi_{1s}(Z_l, \mathbf{r}) , \quad (\text{A2})$$

and so

$$J_i = K \sum_{l,m} c_l c_m \int d^3 q_f M_l^* M_m \delta(e_f - e_i - \Delta E) \quad (\text{A3})$$

or

$$J_i = 2\pi K q_f \sum_{l,m} c_l c_m \int d(\cos\theta) M_l^* M_m , \quad (\text{A4})$$

where θ is the angle between \mathbf{q}_f and \mathbf{K} and the functions M_l^* and M_m have to be evaluated according to Eq. (A1) with $q_f = [2(e_i + \Delta E)]^{1/2}$. Finally, we evaluate the integral in Eq. (A4) by a Gaussian quadrature.

APPENDIX B

In the case of the method 3 (φ_i is the single 1s hydrogenic orbital corresponding to the effective charge Z_i^* (φ_f is the Coulomb wave corresponding to the effective charge Z_f^* ; $Z_i^* \neq Z_f^*$), we can again evaluate the Compton profile via Eq. (A4). However, l and m have here a single value, so that there is no summation. In addition, one has $l=m$, so that the factors coming from $a^{-i\gamma}$ and $(a+b)^{i\gamma}$ of Eq. (12) in Ref. 5 disappear in $M_l^* M_l$ and the integral can be evaluated algebraically. It gives

$$\begin{aligned} J(q_f) = & 32Z_i^{*3} Z_f^* K [1 - \exp(-2\pi Z_f^*/q_f)]^{-1} \exp\{-2Z_f^* q_f^{-1} \tan^{-1}[2Z_f^* q_f / (Z_i^{*2} + K^2 - q_f^2)]\} \\ & \times \{ A_2 Z_f^* (1 + Z_i^{*2}/q_f^2) / [(Z_i^{*2} + K^2 - q_f^2)^2 + 4q_f^2 Z_i^{*2}] \\ & + 2A_3 Z_f^* Z_i^* [(Z_i^{*2} + K^2 - q_f^2)(1 - Z_f^* Z_i^*/q_f^2) - 2Z_i^* (Z_f^* + Z_i^*)] / [(Z_i^{*2} + K^2 - q_f^2)^2 + 4q_f^2 Z_i^{*2}] \\ & + A_4 Z_i^{*2} (1 + Z_f^{*2}/q_f^2) \} , \end{aligned} \quad (\text{B1})$$

where

$$A_n = [(Z_i^{*2} + K^2 + q_f^2 - 2Kq_f)^{1-n} - (Z_i^{*2} + K^2 + q_f^2 + 2Kq_f)^{1-n}] / [(2n-1)Kq_f] . \quad (\text{B2})$$

It can be checked that this expression reduces to Eq. (11) if $Z_i^* = Z_f^*$ and that it gives the following expression for a final plane wave ($Z_f^* = 0$):

$$J(q_f) = (32Z_i^{*5} K q_f / \pi) [(Z_i^{*2} + K^2 + q_f^2)^2 + 4K^2 q_f^2 / 3] / [(Z_i^{*2} + K^2 + q_f^2)^2 - 4K^2 q_f^2]^3 . \quad (\text{B3})$$

This last expression can also be written in the form

$$J(q_f) = 8Z_i^{*5} \{ [Z_i^{*2} + (K - q_f)^2]^{-3} - [Z_i^{*2} + (K + q_f)^2]^{-1} \} / (3\pi) . \quad (\text{B4})$$

In this form it is clear that the maximum J_{\max} is obtained for q_f close to K as stated in Sec. VII A [cf. Eq. (24)] (in fact, it is obtained for q_f slightly larger than K due to the contribution of the second term).

- *Also at Groupe de Chimie Quantique, Laboratoire de Physico-Chimie du Rayonnement, Bâtiment 337, Université de Paris-Sud, 91405 Orsay Cédex, France.
- ¹P. Eisenberger and P. M. Platzman, *Phys. Rev. A* **2**, 415 (1970).
- ²P. Froelich and W. Weyrich, *J. Chem. Phys.* **80**, 5669 (1980); **85**, 1456 (1986); P. Froelich, A. Flores-Riveros, and W. Weyrich, *ibid.* **82**, 2305 (1985).
- ³G. Louprias, J. Chomilier, and D. Guerard, *J. Phys. Lett.* **45** L301 (1984); *Solid State Commun.* **55**, 299 (1985).
- ⁴(a) B. J. Bloch and L. B. Mendelsohn, *Phys. Rev. A* **9**, 129 (1974); (b) L. B. Mendelsohn and B. J. Bloch, *ibid.* **12**, 551 (1975).
- ⁵M. J. Brothers and R. A. Bonham, *J. Phys. B* **17**, 4235 (1984).
- ⁶S. Mukhopadhyaya, S. N. Ray, and B. Taludar, *J. Chem. Phys.* **76**, 2484 (1982).
- ⁷F. Bell, *J. Chem. Phys.* **85**, 303 (1986).
- ⁸L. Mendelsohn and V. H. Smith, in *Compton Scattering. The Investigation of Electron Momentum Distribution*, edited by B. Williams (McGraw-Hill, London, 1977), p. 102.
- ⁹See *Compton Scattering. The Investigation of Electron Momentum Distribution*, Ref. 8, in its entirety.
- ¹⁰R. Currat, P. D. De Cicco, and R. Kaplow, *Phys. Rev. B* **3**, 243 (1971); R. Currat, P. D. De Cicco, and R. J. Weiss, *ibid.* **4**, 4256 (1971).
- ¹¹T. A. Koopmans, *Physica (Utrecht)* **1**, 104 (1933).
- ¹²C. J. Joachain, *Quantum Collision Theory* (Elsevier, Amsterdam, 1975), p. 144.
- ¹³F. B. Van Duijneveldt, IBM Thomas J. Watson Research Laboratory Research Report No. RJ945, 1971 (unpublished).
- ¹⁴T. C. Wong, L. B. Mendelsohn, H. Grossman, and H. F. Wellenstein, *Phys. Rev. A* **26**, 181 (1982).
- ¹⁵*Handbook of Mathematical Functions*, edited by M. Abramowitz and I. A. Stegun (Dover, N.Y., 1972).
- ¹⁶E. Clementi and C. Roetti, *At. Data and Nucl. Data Tables* **14**, 177 (1974).
- ¹⁷After the completion of the calculations presented here a new set of the HF-SCF orbitals of carbon, expanded in a basis of 1s Slater functions, were published [M. Sekiya and H. Tatewaki, *Theor. Chim. Acta* **71**, 149 (1987)]. Thus we have compared the impulse Compton profiles calculated using the four different expansions of the 1s orbitals: Gaussian functions (Ref. 13), 1s and 2s Slater functions (Ref. 16). 1s Slater functions (Sekiya and Tatewaki listed above), and fit of the Gaussian expansion by 1s Slater functions (this work). We have found that the largest relative difference between any pair of the profiles at the maximum is not larger than 10^{-3} , while the effects considered here are of the order of 10^{-1} (see Fig. 4). We conclude that, for the problem considered in this work, any further discussion concerning the best representation of the initial orbital of the electron is irrelevant.